MRS Advances © 2017 Materials Research Society
DOI: 10.1557/adv.2017.120

Processing parameter, microstructure and hardness of Ni base intermetallic alloy coating fabricated by laser cladding

Takeshi Okuno[1], Yasuyuki Kaneno[1], Takuto Yamaguchi[2], Takayuki Takasugi[1], Satoshi Semboshi[3], and Hideki Hagino[2]

[1] Department of Materials Science, Osaka Prefecture University, 1-1 Gakuen-cho, Naka-ku, Sakai, Osaka 5998531, Japan
[2] Technology Research Institute of Osaka Prefecture, 2-7-1 Ayumino, Izumi, Osaka 5941157, Japan
[3] Trans-Regional Corporation Center, Institute for Materials Research, Tohoku University, 1-1 Gakuen-cho, Naka-ku, Sakai, Osaka 5998531, Japan

ABSTRACT

Ni base intermetallic alloy coating was fabricated by laser cladding, controlling the laser power and powder feed rate. Atomized powder of the Ni base intermetallic alloy was laser-cladded on the substrate of stainless steel 304. The hardness and microstructure of the clad layers were investigated by Vickers hardness test, SEM, XRD and TEM observations. The hardness of the cladding layer was affected by the dilution with the substrate; it increased with decreasing laser power and increasing powder feed rate. By optimizing the dilution with the substrate, the cladding layer with an almost identical hardness level to that of the Ni base intermetallic alloy fabricated by ingot metallurgy was obtained. The TEM observations revealed that a very fine-sized microstructure composed of Ni_3Al and Ni_3V was partially formed even in the as-cladded state. After annealing, the two-phase microstructure composed of Ni_3Al and Ni_3V was developed in the cladding layer, resulting in enhanced hardness in the cladding layers fabricated in the majority of cladding conditions.

INTRODUCTION

The present authors have recently developed a new type of two-phase intermetallic alloys composed of Ni_3Al ($L1_2$) and Ni_3V ($D0_{22}$) phases [1-4]. The microstructure is composed of Ni_3Al and Ni solid solution (A1) phases at high temperature, and the Ni solid solution phase is decomposed into (Ni_3Al + Ni_3V) by a eutectoid reaction at a low temperature. The so called dual two-phase microstructure is thus comprised of whole intermetallic (ordered) phases with high structural coherency, leading to high microstructural stability at high temperature. The dual two-phase intermetallic alloys have been found to exhibit excellent strength and hardness at high temperatures due to their stable microstructure, and thereby are expected to be used for high-temperature structural and wear-resistant applications such as high-temperature dies, molds and tools. For wear-resistant applications, coating processes such as thermal spraying and cladding by welding have been practically used. Recently, laser cladding has become widely used as a surface modification processing because of many advantages over other conventional techniques such as thermal spraying and arc welding [5-7]. Laser cladding has a high potential for coatings with low dilution with substrate, minimal distortion and strong metallurgical bonding with substrate, leading to refurbishment or improvement of corrosion, wear and other surface related properties. Also, the laser cladding is convenient for alloying the intermetallics with other

elements, controlling the microstructure and thereby enhancing the properties of intermetallic alloys. However, there has been no report in which the Ni base intermetallic alloy coating composed of Ni_3Al ($L1_2$) and Ni_3V ($D0_{22}$) phases was fabricated by laser cladding although there are some reports in which Ni_3Al intermetallic compound and super alloy coatings were synthesized by laser cladding [6, 7].

In this study, Ni base dual two-phase intermetallic alloys coating was fabricated by laser cladding, adjusting the laser cladding parameters such as laser power and powder feed rate. Atomized powder of the Ni base dual two-phase intermetallic alloys was laser-cladded on the substrate of stainless steel 304. The hardness and microstructure of the coatings were evaluated by Vickers hardness test, SEM, XRD and TEM observations. The relationship between the microstructures and mechanical properties of the coatings was discussed.

EXPERIMENTS

The dual two-phase intermetallic alloys with a particle size of less than 125 μm was used as feeding powder for laser cladding. The blocks of SUS304 stainless steel with a size of 60 mm × 60 mm × 10 mm were used as the substrates. Table 1 shows the chemical compositions of the dual two-phase intermetallic alloys and the substrate.

The laser cladding was conducted in conditions of an argon gas shielding atmosphere, a laser beam size of 5 mm × 5 mm, a scanning speed of 5 mm/s, laser power of 1.0, 1.2, 1.6, and 2.0 kW, and powder feed rates of 6.96, 10.4, 13.9, 17.4, and 20.9 g/min. The powder was fed into the distribution nozzle with an argon gas at a flow rate of 5 l/min.

Microstructures and phase identifications of the laser cladding coatings were investigated by a scanning electron microscope (SEM), X-ray diffraction (XRD) and transmission electron microscope (TEM). Vickers hardness tester with a load of 0.1 kg was used to measure the micro-hardness in the transverse cross-sections of the single clad bead. More than ten points of hardness data were collected and averaged. Two kinds of cladding layers, as-cladded and annealed at 1553 K (1280 °C) for 5 h, were evaluated in this study.

Table 1 Chemical compositions of powder and substrate.

Material	Element (at.%)						
	Ni	Al	V	Nb	Fe	Cr	B*
Powder	Bal.	9	13	3	-	-	0.005
Substrate (SUS304)	8-10.5 (wt.%)	-	-	-	Bal.	18-20 (wt.%)	-

* B is extra numbers (wt.%); the number is not included in the total 100 at.% summing other elements.

RESULTS and DISCUSSION

Microhardness

Fig.1 shows the effects of laser power (kW) and powder feed rate (g/min) on the hardness of the cladding layer. Since the hardness values of the cladding layers fabricated at the power of 1.0 kW and the powder feed rates of 6.96 and 10.4 g/min were widely fluctuated, minimum and

maximum hardness values are shown. The laser claddings were unsuccessful at low laser power such as 1.0 kW. As shown in Fig.1 (a), the largest hardness value (492 HV) was obtained at the laser power of 1.2 kW and the powder feed rate of 17.4 g/min, which is almost the same hardness level as that of the two-phase intermetallic alloys fabricated by the ingot metallurgy. The hardness decreases by raising laser power and reducing powder feed rate because the constituent elements of the substrate (SUS304), such as Fe and Cr, are excessively mingled with the cladding layer. Fe and Cr are expected to destabilize two intermetallic phases Ni_3Al and Ni_3V and alternatively stabilize the A1 phase (Ni solid solution) [8]. In other words, the cladding layers fabricated in the conditions of higher laser power and lower powder feed rate were softened because the microstructure containing much amount of Fe and Cr is not fully ordered. Consequently, in terms of hardness, it appears that the cladding layer was optimized by adopting the laser power of 1.2kW and the powder feed rate of 17.4 g/min. As shown in Fig.1 (b), most of cladding layers were hardened by annealing at 1553 K (1280 °C) for 5 h due to the progressive ordering. The microstructures in the as-cladded state are supposed to be mainly composed of disordered phases (that is, A1 phase) due to a rapid cooling rate after laser irradiation. However, the hardening phases (that is, $L1_2$ or $D0_{22}$ phases) are suggested to be developed by the annealing process. Consequently, heat treatment after laser cladding is beneficial to enhance the hardness of the cladding layer of the present two-phase intermetallic alloys.

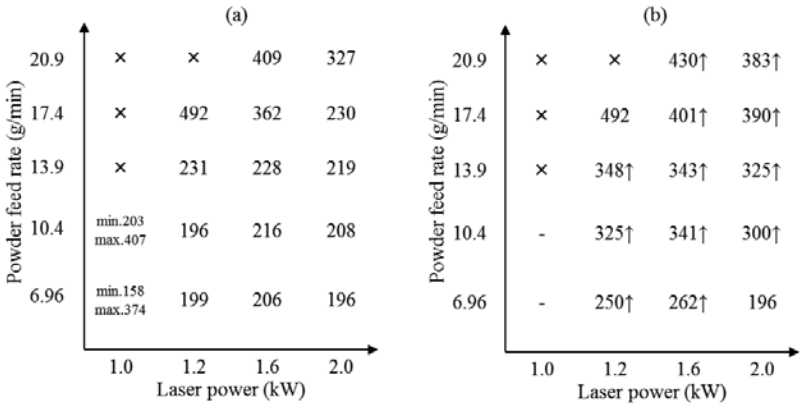

Fig.1 Effects of laser power (kW) and powder feed rate (g/min) on hardness (HV) of the cladding layer (a) as-cladded and (b) annealed at 1553 K (1280 °C) for 5 h. "×" means the unsuccessful cladding layer on the substrate. "↑" means the cladding layers whose hardness values were increased by annealing.

Microstructure observation and phase identification

Fig.2 shows SEM images of the cladding layers fabricated with the laser power of 1.2 kW and the powder feed rate of 17.4 g/min, and with the laser power of 2.0 kW and the powder feed rate of 13.9 g/min. The corresponding XRD profiles are shown in Fig.3. The former cladding layer shows the largest hardness among the prepared specimens while the latter

cladding layer was significantly hardened after annealing at 1553 K (1280 °C) for 5 h. The former cladding layer showed a typical solidification microstructure as shown in Fig.2 (a). The second phase dispersions supposed to be Nb-rich phases are also observed. The XRD measurements exhibited that both Ni_3Al and Ni_3V phases were formed in the as-cladded state (Fig.3 (a)). A detailed analysis clearly shows that the peak at $2\theta = 43 \sim 44°$ was separated into the (111) reflection peak from the Ni_3Al phase and the (112) reflection peak from the Ni_3V phase. Therefore, the observed high hardness for the former cladding layer was possibly due to the presence of (Ni_3Al + Ni_3V) microstructures although they were not resolved in the SEM image. On the other hand, a typical dual two-phase microstructure was formed by annealing at 1553 K (1280 °C) for 5 h (see the inset of Fig.2 (b)). For the latter cladding layer, the microstructure in the as-cladded state showed a featureless matrix containing a smaller amount of second phase dispersions than former cladding layer (Fig.2 (c)). After annealing, most of the second phase dispersions disappeared, resulting in a single-phase microstructure (Fig.2 (d)). It can be understood from Fig.3 (c and d) that the main constituting phase turns from a whole disordered Ni solid solution to (Ni_3Al + Ni solid solution) phases but not to (Ni_3Al + Ni_3V) phases by annealing. Such a microstructural change in the latter cladding layer is due to excess dilution by Fe and Cr from the substrate.

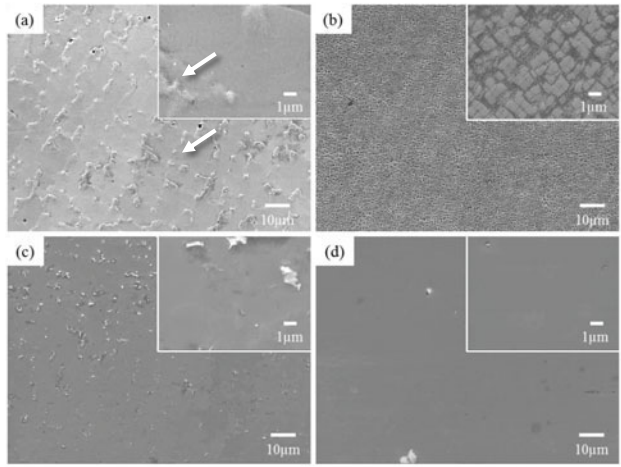

Fig.2 SEM images of microstructures of cladding layers. (a), (c) as-cladded and (b), (d) annealed at 1553 K (1280 °C) for 5 h. (a), (b) fabricated at the laser power of 1.2 kW and the powder feed rate of 17.4 g/min, and (c), (d) fabricated at the laser power of 2.0 kW and the powder feed rate of 13.9 g/min. Arrows indicate Nb-rich second phase dispersions.

The XRD intensities of the (111) and (112) were larger for Figs.3 (b) and (c) but smaller for Figs.3 (a) and (d) than those of the (200) peaks, revealing the presence of the preferential orientations in the cladding layers corresponding to Figs.3 (a) and (d). The different relative XRD intensities are supposed to be due to the inhomogeneous microstructures introduced in the as-cladded state because they were occasionally dependent on the areas projected by X-ray.

Certainly, more careful investigation is required to clarify whether such preferential orientation is present or absent in the present cladding layers.

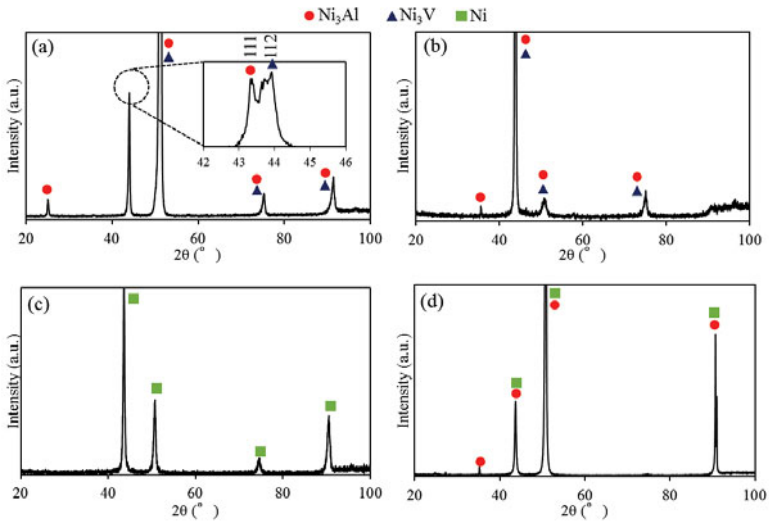

Fig.3 XRD profiles of the cladding layers. (a), (b), (c), and (d) correspond to the same specimens shown in Fig.2.

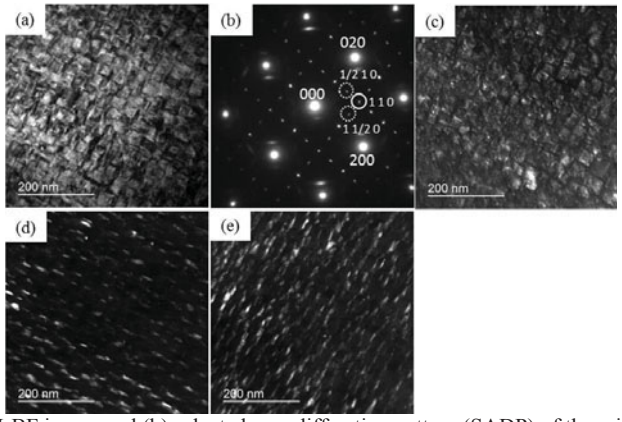

Fig.4 (a) TEM-BF image and (b) selected area diffraction pattern (SADP) of the microstructure of the as-cladded layer at the laser power of 1.2 kW and the powder feed rate of 17.4 g/min. The incident beam direction is $[001]_{Ni3Al}$. (c), (d) and (e) TEM-DF images taken from the diffraction spots 1 1 0, 1/2 1 0 and 1 1/2 0 in the SADP, respectively.

Figs.4 (a) and (b) show the TEM bright field (BF) image and selected area diffraction pattern of the microstructure of the as-cladded layer fabricated at the laser power of 1.2 kW and the powder feed rate of 17.4 g/min, respectively. The two-phase microstructure, which is much finer than that of the two-phase intermetallic alloys fabricated by the ingot metallurgy, was observed. The size of the primary cuboidal phase Ni_3Al in the microstructure of the as-cladded layer is approximately 30-40 nm, which is about one tenth of that of the two-phase intermetallic alloys fabricated by the ingot metallurgy. Figs.4 (c), (d) and (e) show the corresponding dark field (DF) images of the microstructure shown in Fig.4 (a). Here, the DF images were taken by using the extra diffraction spots numbered as 1 ($L1_2$), 2 and 3 ($D0_{22}$) in the selected area diffraction pattern (SADP) in Fig.4 (b). The SADP in Fig.4 (b) is consistent with a typical two-phase microstructure composed of the cuboidal-shaped primary Ni_3Al ($L1_2$) phase and the channel consisting of Ni_3V ($D0_{22}$) and Ni_3Al ($L1_2$) phases. Consequently, the TEM observations revealed that the two-phase ($L1_2$ + $D0_{22}$) microstructure was already formed in the as-cladded state and frozen by successive rapid cooling after laser irradiation.

CONCLUSION

The following results were obtained from the present study.

(1) Ni base dual two-phase intermetallic alloys coating was laser cladded on stainless steel 304 substrate, by adjusting laser power and powder feed rate. The largest hardness (492 HV) of the cladding layer was obtained at the laser power of 1.2 kW and the powder feed rate of 17.4 g/min. This hardness value is almost the same as that of the two-phase intermetallic alloys fabricated by ingot metallurgy. Almost all the cladding layers were hardened by annealing at 1553 K (1280 °C) for 5 h due to the progressive ordering.

(2) The two-phase microstructure composed of Ni_3Al and Ni_3V phases with much smaller scale than those fabricated by the ingot metallurgy was obtained in the cladding layer fabricated at the laser power of 1.2 kW and the powder feed rate of 17.4 g/min. The size of the primary Ni_3Al cuboidal phase in the microstructure of the cladding layer is about 30-40 nm, which is about one tenth of that of the two-phase intermetallic alloys fabricated by the ingot metallurgy.

ACKNOWLEDGMENTS

This work was supported in part by a Grant-in-Aid for Scientific Research (B) (No. 26289263) from the Japan Society for the Promotion of Science (JSPS).

REFERENCES

[1] Y. Nunomura, Y. Kaneno, H. Tsuda, T. Takasugi, Acta Mater. 54 (2006) 851-860.
[2] S. Shibuya, Y. Kaneno, M. Yoshida, T. Takasugi, Acta Mater. 54 (2006) 861-870.
[3] S. Shibuya, Y. Kaneno, H. Tsuda, T. Takasugi, Intermetallics 15 (2007) 338-348.
[4] K. Kawahara, Y. Kaneno, A. kakitsuji, T. Takasugi, Intermetallics 17 (2009) 938-944.
[5] Li YX, Liu Y, Geng HY, Nie DK, J Mater Process Technol. 171 (2006) 405-410.
[6] Y. Yu, J. Zhou, J. Chen, H. Zhou, C. Guo, B. Guo, Intermetallics 18 (2010) 871-876.
[7] T. E. Abioye, A. T. Clare, D. G. McCartney, J. Mater. Process. Technol. 217 (2015) 232-240.
[8] S. Kobayashi, K. Sato, E. Hayashi, T. J. Konno, Y. Kaneno, T. Takasugi, Intermetallics 23 (2012) 68-75.